June 11, 2018

QuakeCoRE Project 2018

Jeff Bayless, Andreas Skarlatoudis, Paul Somerville (AECOM)

We develop a rupture model of a Hikurangi megathrust event, including unilateral rupture with propagation towards the northwest, in accordance with Schellart and Rawlinson (2012). We use the Graves and Pitarka hybrid Irikura method (Pitarka et al. (2018); GP-IM) for developing the source model.

Hikurangi Rupture Geometry

We use the geometric model from GNS Science (Stirling et al., 2012) as the basis for the Hikurangi rupture geometry. The full Hikurangi scenario is composed of three segments: northern (Raukumara), central (Hawke's Bay), and southern (Wairarapa) as identified in Wallace et al., (2009).

The GNS northern and central segments have identical dip angle and down-dip extent. The GNS southern segment has a shallower dipping angle and extends to greater depth. The parameter values for each section are listed in Table 1.

Table 1. Hikurangi rupture properties from GNS (Stirling et al., 2012).

Rupture Scenario	Dip Angle (deg)	Depth to Top of Rupture (km)	Depth to Bottom of Rupture (km)	Length (km)	Strike Angle (deg)	Characteristic Mw
Northern	8.5	5	20	200	209.5	8.3
Central	8.5	5	20	200	209.5	8.3
Southern	10	5	30	224	224.7	8.4
Combined	9.0	5	24	624	Varies	9.0

June 11, 2018

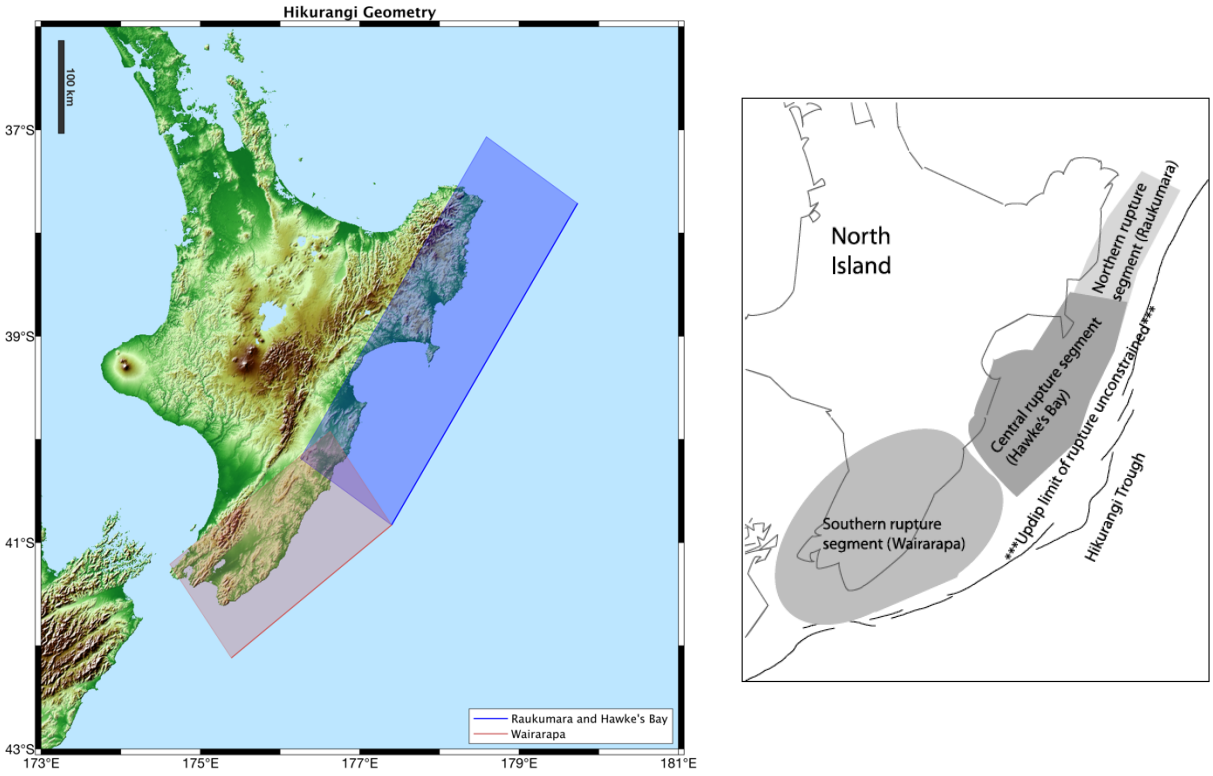

Figure 1. Left: Geometry of the Hikurangi megathrust scenario used for developing the rupture model. The northern and central segments are shown in blue, and the southern segment is shown in red. The solid lines identify the surface traces and the filled areas are the surface projections of the rupture planes. Right: Schematic from Wallace et al., (2009) showing rupture regions for possible subduction events.

June 11, 2018

Seismic Velocity Model

In our 2016 QuakeCoRE project, we developed a generic 1D seismic velocity and density model for the Hawke's Bay region (Figure 2). This model is created by averaging profiles from the Eberhart-Phillips et al. (2010) model sampled within 100km of the Hawke's Bay fault plane, and modified in the upper 1.5 km to have a smooth transition to Vs30=863 m/s. This is the 1D model we adopt for generating the Hikurangi source.

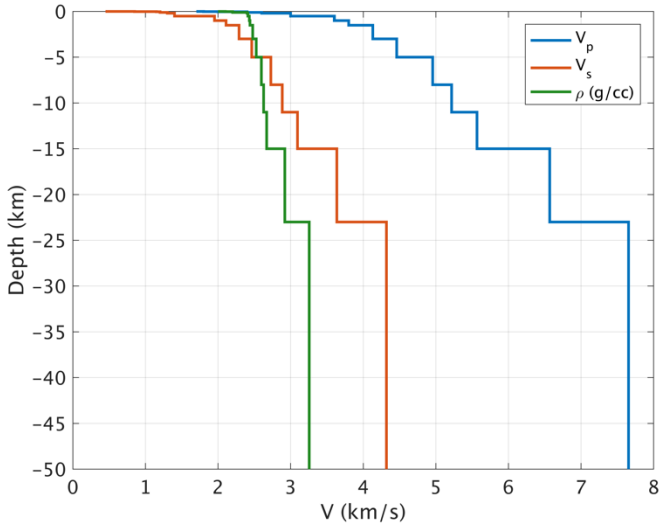

Figure 2. The 1D seismic velocity model used to represent the north island region.

Magnitude Model

We use the Skarlatoudis et al., (2016) self-similar magnitude scaling relationship for subduction earthquakes to determine the scenario magnitude, using the rupture area from GNS. The Skarlatoudis relationship is given as Mw = 3.72 + log10(Rupture Area). Using the combined rupture geometry from Table 1, the total rupture area is 75,816 square km, which yields Mw 8.6.

June 11, 2018

GP-IM Rupture Model

Background

The Pitarka et al. (2018, in preparation) method combines the Irikura and Miyake (2011) asperity-based kinematic rupture generator with the Graves and Pitarka (2015) rupture generation methods for stochastic spatial variability and background slip.

**to do: insert a technical description of the GP-IM method **

We use the GP-IM code version 5.4.0-asp.

A GP source is described by the fundamental scenario parameters: Mw, strike, dip, rake, fault dimensions, hypocenter location, and fault location. In addition to the scenario parameters, several code parameters must be specified. The scenario and code parameters we specified in the GP-IM code are given in Table 2.

Modifications to GP-IM for Subduction Events

Up to now, the model input parameters have been only calibrated for crustal earthquakes. Rob Graves and Arben Pitarka have not used the model extensively with subduction events. Based on our communication with them, we have made the modifications to the model described in this section. They both recommend that the model should be validated with recordings from subduction earthquakes.

The standard GP rupture model generator uses relationships for crustal earthquakes for scaling the corner wavenumbers. We use the Skarlatoudis et al. (2016; Equation 4) scaling for the corner wavenumbers in the along strike and down-dip direction. This model was developed for great interface subduction earthquakes and used the Somerville et al. (1999) approach for crustal earthquakes. The corner wavenumbers have self-similar scaling with Mw. Using this wavenumber model with a Mw8.6 scenario introduces smoother background slip than the crustal earthquake wavenumber relationships.

Wirth et al (2017) examined the deltaT perturbations to the rupture times (Equation 6 of Graves and Pitarka, 2016) on the 2003 Tokachi-oki M8.3 event. They found that the

perturbations were too large for large magnitude earthquakes, and led to a significant reduction in ground motion. Rob Graves discussed this with the authors and concluded the parameterization for deltaT scaled too strongly with increasing magnitude. He recommended we implement the following magnitude dependence for deltaT into his code: tsfac_main = max { -0.5 * 1.0e+09 * Mo^(1/3) - 0.1, -2.0 }, where tsfac_main is the standard error of deltaT.

Other GP parameters Rob Graves suggested we can modify are the parameters that control the average rupture speed and rise time: "rvfrac" and "risetime_coef", respectively. In this case, "average" means the average as computed across the entire fault, but there can be significant spatial variation over the fault.

Rob Graves also wrote (pers. comm. April 19, 2018): "For rupture speed, the default value is rvfrac=0.8, which means the average rupture speed will be at 0.8*local_Vs (Vs at the subfault location). For risetime_coef, the default value is risetime_coef=1.6, and this is used in the code to set the actual rise time using the relationship from Somerville et al. The rise time is the total duration of our Kostrov-like slip-rate function. Most of the strong motion is radiated in the beginning pulse of this function which has a duration of about 20% of the total rise time duration."

Rob Graves and Arben Pitarka recommended trying variations of the 2 average parameters (rvfrac & risetime_coef) and the rupture time perturbations first. Future steps may involve investigating any depth dependence of the weak zone.

Magnitude-Area-Asperity Area Relationship

Arben Pitarka has helped us communicate with Tokyo University and Georesearch Institute about the Irikura recipe for subduction zone earthquakes (pers. comm. May 4, 2018). There is no final recipe for subduction zone earthquake rupture models in Japan yet, but the following information was provided.

Murotani proposed the relationships between the magnitude and fault area, and the magnitude and asperity area (Murotani et al., 2008; Figure 2a, c). Tajima also proposed the relationships between the magnitude and fault area assuming the second stage (Tajima et al., 2013; Figure 2a). Estimates for the large slip area are provided from inversion analysis (solid symbols) and from EGF forward modeling (empty symbols). They show the relationships between the magnitude and fault width with saturation (Tajima et al., 2013; Figure 4). The width saturation relationship is not validated yet.

The Murotani et al., (2008) relationships for combined asperities with respect to seismic moment for plate-boundary earthquakes are shown in Figure 3.

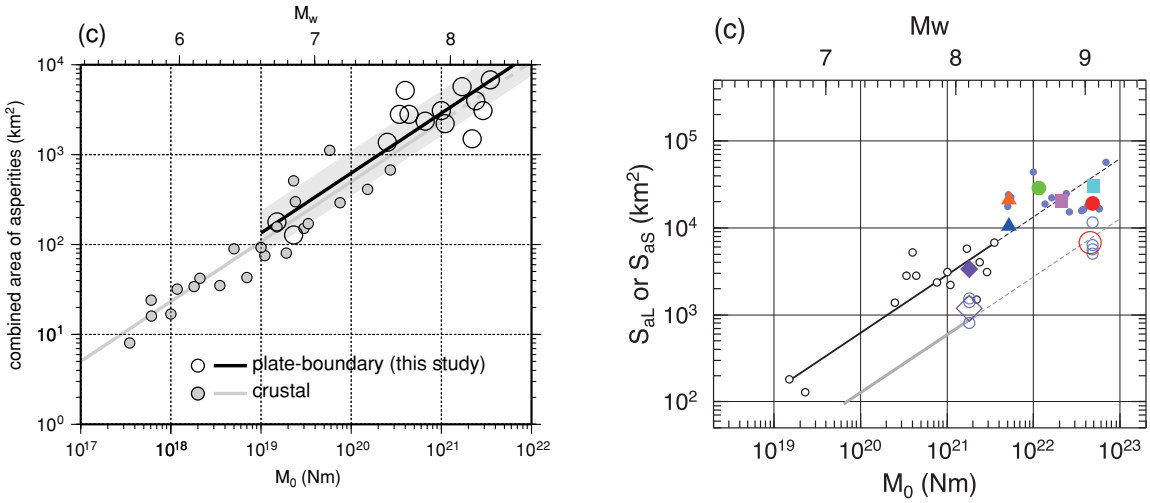

Figure 3. Left: from Murotani et al., (2008), the scaling relationship of combined asperities with respect to seismic moment for plate-boundary earthquakes (heavy line). Right, from Tajima et al., (2013), the same relationship. The dark solid line is the Murotani et al., (2008) relationship, extended with the dashed dark line to larger magnitudes and with additional data (symbols).

We spoke with Hiroe Miyake at the SSA Annual meeting in Miami, and she provided the following information about adapting the Irikura and Miyake (2011) method for large subduction earthquakes (per. comm. June 7, 2018):

> *For Mw 7-8 class subduction earthquakes, Long-period: 3 MPa for average stress drop, size of asperity is 20%, 15 MPa for stress drop of asperities.*
> *Short-period: 3 MPa for average stress drop, size of SMGA is 10%, 30 MPa for stress drop of SMGAs.*
>
> *If you plan to try Mw 9 class subduction earthquakes, e.g., Short-period would be 3 MPa for average stress drop, size of SMGA is 5%, 60 MPa for stress drop of SMGAs. You can adjust percentage of SMGAs to fit the data or GMPEs.*
>
> *We can just keep stress drop of SMGAs = average stress drop / percentage of SMGA size following the Madariaga (1979) equations.*

In the GP-IM method, the stress drop is not an explicit input parameter used to describe the source, because the GP and IM methods use very different techniques in computing the high frequency ground motions. The ratio of asperity to background slip is controlled by the GP-IM input parameter A0, described below. We define the scenario SMGA areas based on the advice from Hiroe Miyake (above) and on the extended Murotani et al., (2008) relationship. Hiroe Miyake suggested using 10% of total rupture area for short-period SMGAs and 20% of the total rupture area for long-period SMGAs

(Mw 7-8 class earthquakes.) In GP-IM, we specify the SMGA areas for both long and short periods using the same model, therefore we average these values to get a ratio of 15%. We checked this value with the ratio suggested by Murotani et al., (2008). For a M8.6 subduction zone earthquake, the Murotani et al., (2008) rupture area and SMGA area are approximately 1.0E5 and 1.5E4 square km, respectively, with a ratio of 15%. Using this ratio, and with the Hikurangi scenario rupture area of 7.58E4 square km, we calculate a SMGA area of 1.14E4 square km.

Final Parameter Specifications

In Table 2 we list all the scenario, GP-IM code, and asperity parameter values prescribed in developing the Hikurangi rupture model.

The total asperity area, 1.14E4 square km, is split into four asperities, as shown in Figure 4 and listed in Table 2. In Table 2, the asperity properties are given in the following form: [A0 X1 Y1 X2 Y2], where A0 is the relative asperity strength (related to the ratio of asperity to background slip), X1 and Y1 are the distances along strike and down dip to the top left corner of the asperity, measured from the top center of the fault. X2 and Y2 are the same distances but for the bottom right corner of the asperity.

We have specified 3 asperities with area 1,805 square km (each approx Mw 7.0) and one with 5,984 square km (approx. Mw 7.5), all using approximate aspect ratios consistent with the overall rupture. They are placed in deeper portion of the rupture plane, consistent with the assumptions used in Wirth et al., (2017).

Table 2. Scenario, GP-IM code, and asperity parameter values prescribed in the rupture model development.

GP Scenario Parameters		
	Value	**Comment**
Moment Magnitude	8.6	Scaling from Skarlatoudis et al. (2016)
Fault Strike (deg)	209.5, 224.7	Northern segment, Southern segment
Rupture Length (km)	624.0	Total length of both segments
Rupture Width (km)	121.5	
Top-Center Lat, Lon (deg)	-40.1448, 177.9346	Reference coordinate.
Hypocenter Lat, Lon (deg)	-41.6114, 175.2347	Southern segment
Hypocenter Location Along Strike (km)	300.0	Measured from the top-center, along strike (including bend).
Hypocenter Location Down Dip (km)	60.0	Measured from the top of rupture, along dip.
Average Rake (deg)	90.0	Sub-fault rake angles include perturbations.
Fault Dip (deg)	9.0	
Depth to Top of Rupture (km)	5.0	
Dx, Dy (km)	1.0, 1.0	Dimensions of the sub-faults.
Seed	5481191	For random number generator.
GP-IM Code (v5.4.0-asp) Parameters		
SLIP1_SCOR	0.999	Controls the amount of stochastic variability in the slip distribution.
MASTER_RVFRAC	0.80	Vr/Vs ratio. Vs is the local shear wave velocity given in the 1D crustal model.
EXTEND_FACTOR	1.25	Relic code parameter.
RISETIME_COEF	1.95	Coefficient that controls the rise time, where the actual rise time is calculated as: RISETIME_COEF *1.0e-09*exp(log(Moment)/3.0);
RUP_DELAY	0.0	No rupture delay.
SLIP_COV	0.85	Controls the slip distribution roughness.
DT	0.0125	Time step in the source time function.
ALPHA_ROUGH	0.0	Controls the fault geometry roughness.
TSFAC_MAIN	Relationship given above	Magnitude dependent perturbations to the rupture times.
Kx, Ky	Skarlatoudis et al., (2016)	Corner spatial wavenumbers
GP-IM Asperity Parameters		
Asperity Number	1	
[A0 X1 Y1 X2 Y2]	2.1 112 75 288 109	See description in text.

Size (km^2)	5,984	176 x 34 km, Mw 7.5
Asperity Number	2	
[A0 X1 Y1 X2 Y2]	2.1 -38 90 57 109	
Size (km^2)	1,805	95 x 19 km, Mw 7.0
Asperity Number	3	
[A0 X1 Y1 X2 Y2]	2.1 -161 65 -66 84	
Size (km^2)	1,805	95 x 19 km, Mw 7.0
Asperity Number	4	
[A0 X1 Y1 X2 Y2]	2.1 -284 78 -189 97	
Size (km^2)	1,805	95 x 19 km, Mw 7.0

Multi-Segment Modification

The GP-IM method generates ruptures for single-segment planar faults. To accommodate the multi-segment geometry of the Hikurangi, we took the following approach. First, we specify one source description for the total Mw event, using the strike direction from the northern and central segments. We use GP-IM to create the SRF file. The resulting SRF file is single-segment planar. Then, the coordinates of the SRF corresponding to the southern segment are transformed such that the subfaults on the southern segment are located as shown in Figure 1. The result is a single SRF file with two planar segments, as shown in Figure 1.

This procedure results in a full Hikurangi rupture scenario with a single Mw, no slip velocity discontinuity, and a single hypocenter. The radiation pattern and rake continuity are maintained between the segments.

Rupture Model Summary

The Hikurangi megathrust scenario rupture model we developed is shown in Figure 4. This figure shows the slip on the fault plane in shades of red, with rupture initiation contours (black lines) at 10 s intervals. The break between the northern and southern segments is identified by the dashed blue line. The maximum slip over the rupture planes is approximately 14 m, and the average slip is approximately 3.5 m. Both of these values agree with the scaling observed by Tajima et al., (2013), shown in Figure 5, and with Skarlatoudis et al. (2016; Figure 3).

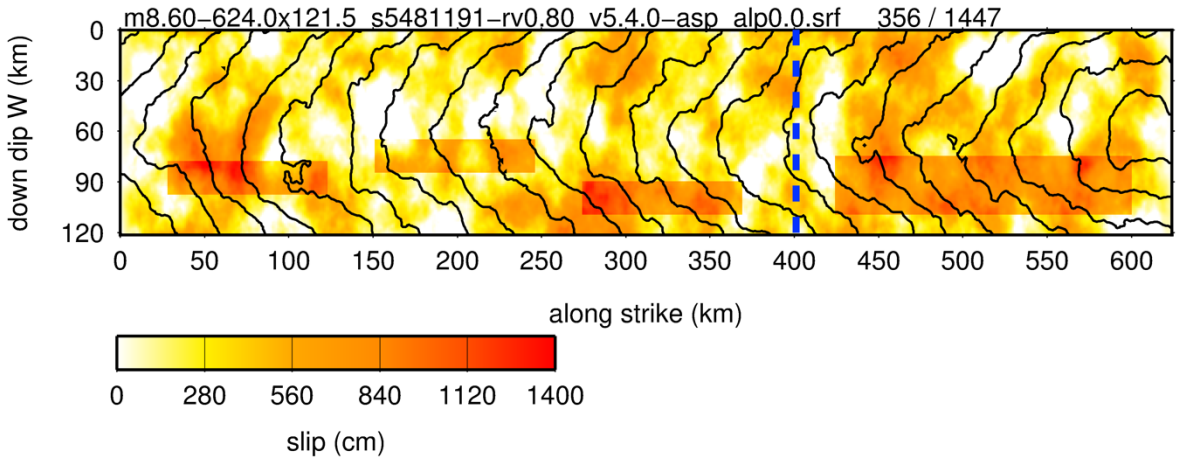

Figure 4. The rupture model of the Mw8.6 Hikurangi scenario developed. The slip is indicated by the red shading, contours of the rupture initiation times with 10 s intervals given by black lines, and the northern and southern segment boundary is given by the blue dashed line.

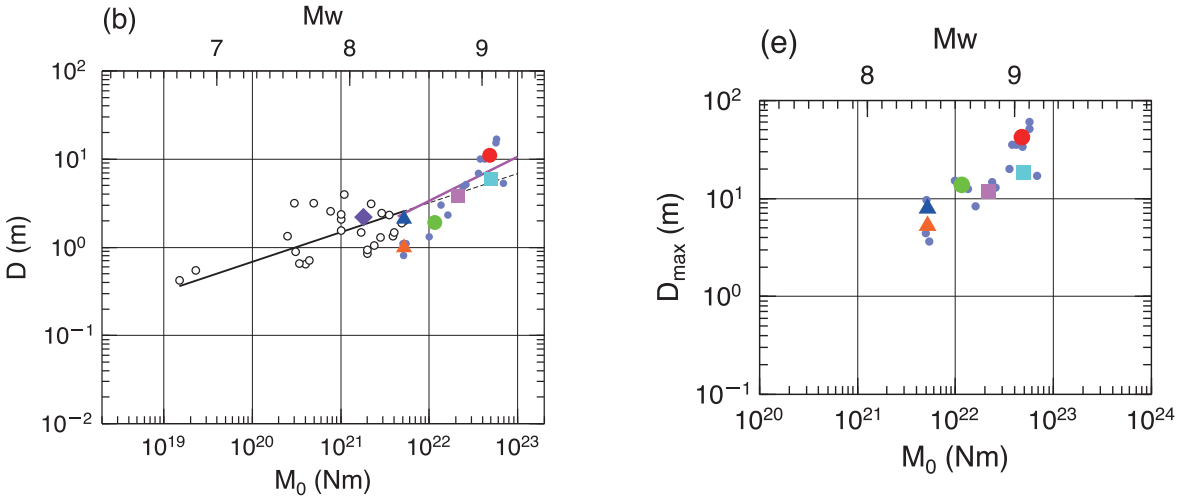

Figure 5. Left: From Tajima et al., (2013), the scaling relationship for average slip with seismic moment. Right, from Tajima et al., (2013), the scaling of maximum slip with seismic moment for plate-boundary earthquakes.

Acknowledgements

Thanks to Rob Graves and Arben Pitarka, both of whom we could not have performed this study without. Arben provided us his GP-IM code along with instructions, verification tests, and helped us communicate with GRI about how to handle subduction earthquakes. Rob provided invaluable information about the GP rupture model generator, including guidance on parameters to modify for subduction events. Both Rob and Arben provided continuous support. We also thank Hiroe Miyake for her help with defining the asperities.

References

Eberhart-Phillips, D., Reyners, M., Bannister, S., Chadwick, M., Ellis, S. (2010). Establishing a Versatile 3-D Seismic Velocity Model for New Zealand. Seismological Research Letters Nov 2010, 81 (6) 992-1000; DOI: 10.1785/gssrl.81.6.992

Graves, R. and Pitarka, A. (2015). Refinements to the Graves and Pitarka (2010) Broadband Ground-Motion Simulation Method. Seismological Research Letters. 86. 10.1785/0220140101.

Irikura, K., & Miyake, H. (2011). Recipe for Predicting Strong Ground Motion from Crustal Earthquake Scenarios. Pure and Applied Geophysics, 168(2011), 85–104. doi: 10.1007/s00024-010-0150-9

Murotani S., Miyake, H., and Koketsu, K. (2008). Scaling of characterized slip models for plate-boundary earthquakes. Earth Planets Space, 60, 987-991.

Pitarka et al. (2018) In preparation

Schellart and Rawlinson (2012). Global correlations between maximum magnitudes of subduction zone interface thrust earthquakes and physical parameters of subduction zones. Physics of the Earth and Planetary Interiors. Volume 225, December 2013, Pages 41-67

Skarlatoudis, A.A., Somerville, P.G., Thio, H.K. (2016). Source-scaling relations of Interface Subduction Earthquakes for Strong Grounf Motion and Tsunami Simulations. Bulletin of the Seismological Society of America, 106(4): 1652-1662; doi: 10.1785/0120150320

Somerville, P. G., K. Irikura, R. Graves, S. Sawada, D. Wald, N. Abrahamson, Y. Iwasaki, T. Kagawa, N. Smith, and A. Kowada (1999). Characterizing crustal earthquake slip models for the prediction of strong ground motion, Seismol. Res. Lett. 70, 59–80.

Stirling, M.W.; McVerry, G.H.; Gerstenberger, M.C.; Litchfield, N.J.; Van Dissen, R.J.; Berryman, K.R.; Barnes, P.; Wallace, L.M.; Villamor, P.; Langridge, R.M.; Lamarche, G.; Nodder, S.; Reyners, M.E.; Bradley, B.; Rhoades, D.A.; Smith, W.D.; Nicol, A.; Pettinga, J.; Clark, K.J.; Jacobs, K. 2012 National seismic hazard model for New Zealand : 2010 update. Bulletin of the Seismological Society of America, 102(4): 1514-1542; doi: 10.1785/0120110170

Tajima, R., Matsumoto, Y., and Si, H. (2013). Comparative Study on Scaling Relations of Source Parameters for Great Earthquakes on Inland Crusts and on Subducting Plate-Boundaries. Journal of the Seismological Society of Japan, 2nd ser. Vol 66, pp 31-45. doi: 10.4294/zisin.66.31

Wirth, E.A., Frankel, A.D., Vidale, J.E. (2017). Evaluating a Kinematic Method for Generating Broadband Ground Motions for Great Subduction Zone Earthquakes: Application to the 2003 Mw 8.3 Tokachi-Oki Earthquake. Bull. Seis. Soc. Of Am. Vol 107, No 4, pp 1737-1753. doi: 10.1785/0120170065